Hindawi Publishing Corporation
International Journal of Polymer Science
Volume 2015, Article ID 293981, 9 pages
http://dx.doi.org/10.1155/2015/293981

Research Article

Chemical Functionalization and Characterization of Cellulose Extracted from Wheat Straw Using Acid Hydrolysis Methodologies

Chemar J. Huntley,[1] Kristy D. Crews,[1] and Michael L. Curry[1,2]

[1]*Department of Materials Science and Engineering, Tuskegee University, Tuskegee, AL 36088, USA*
[2]*Department of Chemistry, Tuskegee University, Tuskegee, AL 36088, USA*

Correspondence should be addressed to Michael L. Curry; currym@mytu.tuskegee.edu

Received 17 September 2014; Revised 15 December 2014; Accepted 15 December 2014

Academic Editor: Cornelia Vasile

The nonuniform distribution of cellulose into many composite materials is attributed to the hydrogen bonding observed by the three hydroxyl groups located on each glucose monomer. As an alternative, chemical functionalization is performed to disrupt the strong hydrogen bonding behavior without significant altering of the chemical structure or lowering of the thermal stability. In this report, we use wheat straw as the biomass source for the extraction of cellulose and, subsequently, chemical modification via the Albright-Goldman and Jones oxidation reactions. X-ray diffraction analyses reveal that upon oxidation a slight change in the cellulose polymorphic structure (CI to CII) can be observed when compared to its unmodified counterpart. Scanning electron microscopy analyses show that the oxidized cellulose structure exhibits fiber-like crystals with lengths and diameters on the micrometer scale. Thermal analyses (differential scanning calorimetry and thermogravimetric analysis) show an increase in the thermal stability for the modified cellulose at extremely high temperatures (>300°C).

1. Introduction

Interests in the use of cellulose in the development of renewable and sustainable technology that is carbon neutral, nonpetroleum based, and biodegradable and has minimal negative impacts on the environment have increased in every lab across the globe. Although cellulose has unique physicochemical properties and has been used as reinforcement components in composites, the hydrophilic nature of cellulose introduces severe limitations for its use in technological applications. More specifically, this is due to the nonuniform distribution of the cellulose crystals into the polymer matrix, which is triggered by negative surface charges and the introduction of void areas caused by inaccurate cellulose dispersion and incompatibility between the two phases [1]. Furthermore, in addition to the elimination of defects associated with the hierarchical structure, cellulose extraction methodologies, such as the use of strong mineral acids, can significantly influence the dispersion and stabilization of cellulose crystals obtained from various biomass sources [2]. Literature reports indicated that the use of sulfuric acid is the most effective hydrolysis process in terms of cellulose stability and dispersibility; however, it is known to produce the most stable cellulose particles with a corresponding negative surface charge via esterification reactions [3]. One solution for decreasing inaccurate dispersion of cellulose crystals into polymer matrices due to the induced negative surface charges and incompatibility, as well as aggregation, is through chemical functionalization [1]. That is, through controlling the nature of the surface interactions between the cellulose crystals and host matrix, the incompatibility and low dispersibility of the cellulose crystals throughout the host matrix can be modified.

In the case of cellulose functionalization, the reactivity nature is primarily dependent upon the hydroxyl groups. However, cellulose reactions are governed by hydrogen bonding and steric hindrance [4], as well, and, in return, along with the polymer-analogous concept, assist in determining the

Table 1: The cellulose, hemicellulose, and lignin content of various agricultural waste materials.

Agricultural waste material	Cellulose (%)	Hemicellulose (%)	Lignin (%)
Nut shells	25–30	25–30	30–40
Corn cobs	45	35	15
Grasses	25–40	35–50	10–30
Paper	85–99	0	0–15
Leaves	15–20	80–85	0
Newspaper	40–55	25–40	18–30
Cotton seed hairs	80–95	5–20	0
Wheat straw	**35–40**	**30–35**	**10–15**

best functionalization techniques. The polymer-analogous concept was introduced by Staudinger and Daumiller and states that macromolecules are capable of undergoing similar reactions to that of low-molecular compounds. Still, the supramolecular structure stimulates the determination of the degree of conversion, functional group distributions, and the rate of reaction, essential for parameter determination in functionalization techniques [5].

One form of cellulose functionalization reaction essential in introducing carbonyl groups at the C2, C3, and C6 positions of cellulose is oxidation. Numerous oxidation reactions exist, yet interest in the Albright-Goldman and Jones oxidation reactions has been limited. The Albright-Goldman oxidation specifically targets sterically hindered functional groups present in the cellulose supramolecular structure, but both oxidation techniques are capable of producing aldehydes, carboxylic acids (more present in the Jones oxidation), and ketones [6]. Thus, in order to understand how these nonconventional techniques affect the common steric hindrances of cellulose when compared to other oxidation methods (i.e., TEMPO-mediated oxidation) [2], detailed studies should be undertaken. Therefore, the aims of this report are to (1) chemically functionalize cellulose in order to introduce aldehydes and ketones on the primary and secondary alcohols without any major structural rearrangements using the Albright-Goldman and Jones oxidation reactions, (2) decrease the hydrophilic nature of the polymer, and (3) increase the thermal stability.

2. Experimental

2.1. Materials. ACS reagent grade agents purchased from Sigma-Aldrich were used as received. Acetic acid, acetone, nitric acid, sodium chlorite, sodium hydroxide, and sulfuric acid for cellulose synthesis were purchased from Sigma-Aldrich. For cellulose modification, acetic anhydride, ammonium hydroxide, dimethyl sulfoxide, silver nitrate, and sodium dichromate were purchased from Sigma-Aldrich. Wheat straw was purchased from Georgia. Table 1 gives insight into the cellulose, hemicellulose, and lignin content of wheat straw versus other agricultural waste materials.

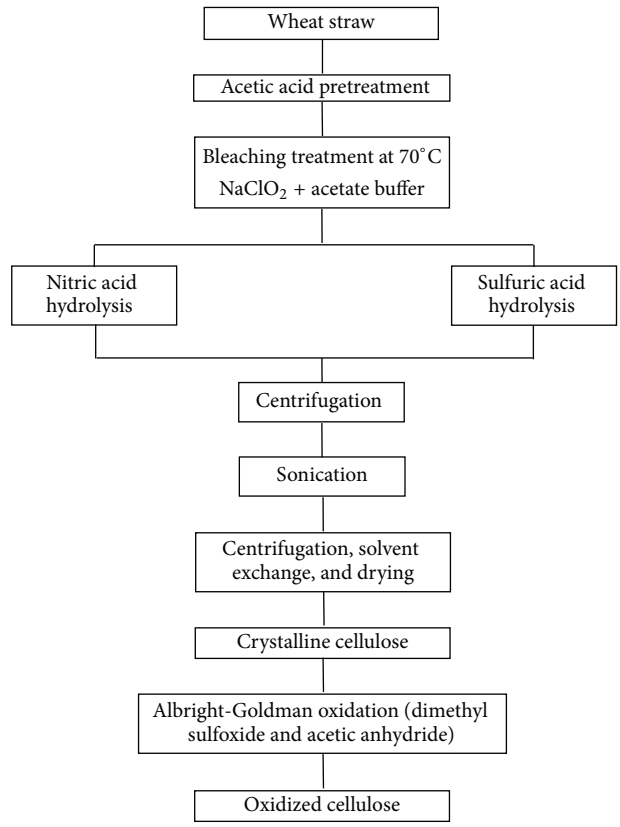

Figure 1: The isolation and chemical functionalization methodology for the crystalline cellulose isolated from wheat straw.

2.2. Isolation of Crystalline Cellulose. In this paper, solutions were prepared in the following concentrations: 90 wt.% acetic acid, 9 wt.% sodium chlorite, 58 vol.% acetic acid and 42 vol.% sodium hydroxide buffer solution, 32 vol.% nitric acid, and 32 vol.% sulfuric acid. Wheat straw was subjected to fractionation by refluxing in the presence of an acetic acid solution for phenolic and hemicellulose hydrolysis at a duration of 2 hours (see Figure 1). Subsequently, the mixture was filtered using Buchner filtration with Whatman # 1 filter paper and washed with hot distilled water to rid the wheat straw of remaining acid. Bleaching was carried out using a sodium chlorite solution in an acetic acid and sodium hydroxide buffer system at approximately 78°C for 2 hours, producing the strong oxidizing agent chlorous acid. This bleaching step ensured the release of cellulose from lignin and remaining hemicellulose. The product was filtered using the previously stated filtration method. The resulting cellulose was treated with the 32 wt.% strong acid solutions—nitric and sulfuric acids—for 24 hours, specifically targeting the voids of the amorphous regions. Afterwards, purification and neutralization of the resulting crystalline cellulose were performed by centrifuging 3–6 times at 2500 rpm for 30 minutes with the addition of fresh distilled water after each time. To avoid aggregation, the product was sonicated on an ice bath for 4 hours, centrifuged 3 additional times with the prior conditions, and allowed to settle for 24 hours. The distilled water was decanted from the product and replaced

with acetone for drying. Centrifugation was performed at 1000 RPM for 10 minutes. Afterwards, fresh acetone was added. The process was repeated 3 times and allowed to settle for 24 hours. Samples were dried at approximately 70°C in a vacuum oven.

2.3. Chemical Functionalization and Tollens' Test. A solvent exchange from acetone to 10.00 mL of dimethyl sulfoxide was completed for samples of 1.00 to 2.00 grams of cellulose. The Albright-Goodman oxidation was performed according to Albright and Goldman [7]. Using a test tube, a small amount of dried, oxidized cellulose was mixed with a Tollens' reagent of 50 mL of 0.1 M silver nitrate, ammonium hydroxide, and 25 mL of 0.8 M sodium hydroxide [8].

2.4. Characterization of Crystalline Cellulose

2.4.1. Fourier Transform Infrared Spectroscopy. Fourier transform infrared (FTIR) spectra were collected for the modified and neat cellulose. FTIR analyses were performed using a Shimadzu 8400S FTIR spectrometer. The data was collected and analyzed using IRSolution software and reported literature findings for crystalline cellulose.

2.4.2. X-Ray Diffraction Spectroscopy. Crystal structures of the formed cellulose were analyzed using a Rigaku D/MAX 2200 X-ray diffractometer with a diffracted beam graphite monochromatic running on Cu Kα radiation. Analysis was performed from 0° to 80° of 2θ angle at a rate of 5 degrees per minute and a sample width of 0.02.

2.4.3. SEM Imaging of Cellulose Crystals. Electron microscopy images of cellulose were carried out using a Zeiss EVO 50VP scanning electron microscope. The crystalline cellulose was analyzed by sputter coating with copper using a 550X sputter coating device. The Zeiss EVO 50VP was operated at an acceleration voltage of 20 kV. For each sample, different parts of the grid were used to determine both average shape and size distributions.

2.4.4. Tollens' Test. Tollens' test, or the silver mirror test, was synthesized by the German chemist Bernhard Tollens. The test verifies the presence of aldehydes by using silver (I) to reduce sugar, subsequently leading to the oxidation of an aldehyde to a carboxylic acid. As a result, a grey or silver precipitate is produced after a series of color changes. However, in the presence of a ketone, a precipitate is not produced, and the solution remains colorless. The reagents involved in the mixture are aqueous silver nitrate with aqueous sodium hydroxide [9].

2.5. Thermal and Stability Characterization of Cellulose Extract

2.5.1. Modulated Differential Scanning Calorimeter. Initial identification of the decomposition temperature and melting point of cellulose from wheat straw was analyzed using a TA Instrument Q2000 Differential Scanning Calorimeter. Samples of 10–13 mg were pressed in Hermetic pans and performed from 30°C to 400°C at a rate of 5 degrees per minute.

2.5.2. Thermogravimetric Analysis. Thermal stability of the cellulose was determined using TA Instrument Q500 Thermogravimetric Analyzer. Analysis was performed on samples of 10–15 mg in an oxygen atmosphere from 30°C to 550°C at a rate of 5 degrees per minute.

3. Results and Discussion

3.1. X-Ray Diffraction Analysis (XRD). The polymorphic structure of the nonmodified and modified cellulose crystals extracted via sulfuric and nitric acid hydrolyses was determined using XRD analysis (see Figures 2(a)–2(d)). As can be observed in Figure 2(a), cellulose extracted under nitric acid conditions and modified using the Albright-Goldman reaction method exhibits crystalline properties of cellulose I_α and I_β (CI_α and CI_β), as well as cellulose II (CII) polymorphs. Figure 2(b) exhibits XRD peaks around 15°, 22°, and 35° 2θ indicating that the nitric acid extracted cellulose crystals adopt a CI structural formation [10]. However, upon oxidation of the nitric acid cellulose crystals, a new, sharp XRD peak can be observed at around 20.3° 2θ; this peak corresponds to the formation of a CII polymorphic cellulose crystal structure [10]. Using XRD data simulation software, further support was provided for the presence of the CII polymorph based on the appearance of the new XRD peak at 20.3° 2θ (see Figure 3) [11]. Hence, although complete conversion between the polymorphic structures remains incomplete [12] and CII structures are generally obtained using mercerization techniques with set parameters [5], the presence of the CII crystal structure proves significant for a possible CI to CII conversion mechanism under the Albright-Goldman oxidation reaction.

However, in the case of cellulose extraction under sulfuric acid conditions, modified samples of cellulose using the Albright-Goldman method reveal a different crystal orientation effect when compared to the unmodified nitric and sulfuric acid extracted and modified nitric acid extracted cellulose crystals. The majority of the crystalline peaks present when compared to the unmodified sample are clearly lower in intensity. That is, XRD peaks located at 7.5°, 11.7°, 15°, 23°, and 35° 2θ for the sulfuric acid extracted cellulose are no longer distinct, observable features within the XRD spectrum of the cellulose that has been extracted using sulfuric acid hydrolysis and modified through the Albright-Goldman reaction mechanism. This could be explained through the sacrifice in structure integrity due to the thermodynamic nature of the initial surface groups' alterations during the acid hydrolysis process; however, further investigations are warranted to determine the exact mechanism promoting the structural difference.

3.2. Fourier Transform Infrared Spectroscopy (FTIR) and Tollens' Test. To monitor the structural change in peripheral

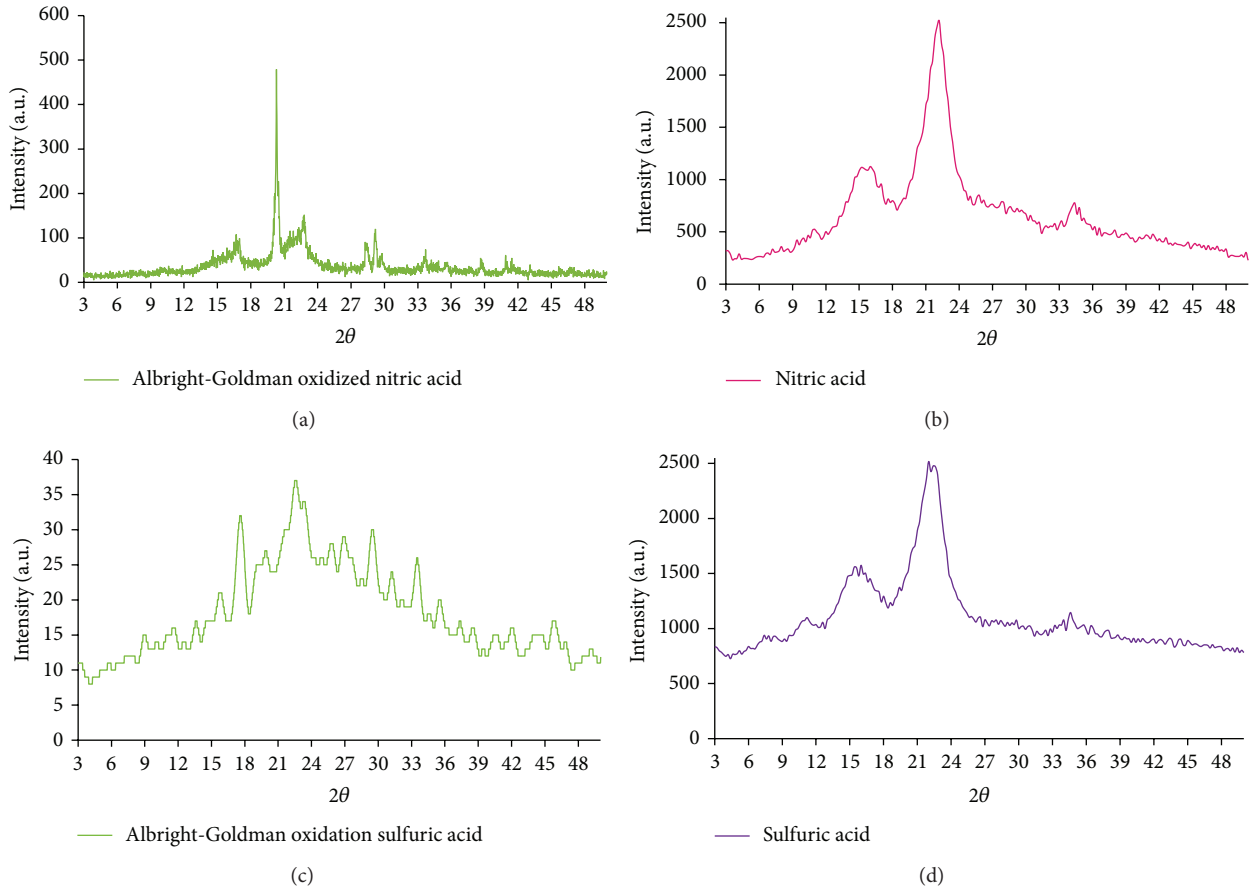

FIGURE 2: X-ray diffraction patterns of nitric acid extracted cellulose (a-b) and sulfuric acid extracted cellulose (c-d) and their Albright-Goldman modified counterparts.

OH groups occurrence after the Albright-Goldman oxidation reaction, the presence and absence of distinct functional groups were determined using FTIR analysis (see Table 2). Based on the arrangement of the polymer and history and source of the waste product, chemical modification tends to occur quicker on the surface of crystallites and disordered regions [13]. In Figures 4(a)-4(b), sulfuric and nitric acid samples display similar results. OH stretches are observed in the 4000–2995 cm^{-1} range with a broader peak and greater intensity apparent in the Albright-Goldman oxidized (sulfuric and nitric acids extracted modified) cellulose, suggesting the scission of the hydrogen bonds [13]. However, it is noted that the modified cellulose shown in Figure 4(a) shows a shift in its OH-stretching vibrations to a slightly lower wavenumber. One may speculate that this could be due to the incomplete removal of hemicelluloses or even lignin during the extraction process, but verification of the removal of these impurities can be proven through the lack of peaks observance at 1735 cm^{-1}, 1600 cm^{-1}, 1515 cm^{-1}, 1426 cm^{-1}, and 1384–1346 cm^{-1}. Furthermore, the modified extracted cellulose FTIR spectra in both the nitric and sulfuric acids cases, Figures 4(a) and 4(b), respectively, reveal that the intensity of the C=O, H–O–CH_2, H–O–H bending of absorbed water around 1640–1623 cm^{-1} is greater in comparison to the unmodified cellulose systems [8, 14]. That is, upon chemical functionalization a greater amount of water is absorbed, as well as the introduction of the C=O onto the primary and/or secondary hydroxyl groups on the structure. This can be explained by the possible replacement of the OH groups for the unmodified acid extracted cellulose when compared to the modified. Since partial substitution of the O-H functional groups are replaced with either nitro or sulfate groups during the acid hydrolysis process, and CHO_2 or CO_2 groups in the case of the modified, a change may be induced in the hydrophilic nature of the cellulose structure comparatively [13].

Further support for partial oxidation of the cellulose structure during the modification can be seen using Tollens' test; see Figure 5. This qualitative test is used to verify the presence of aldehydes, which will occur on carbon 6 (C6) of the cellulose structure. In short, in the presence of aldehydes, Tollens' reagent will go through a specific color change (Figures 5(a)–5(c))—golden yellow, brown, and dark and cloudy gray—before the formation of silver apparently forms on the walls of the test tubes (see Figures 5(a)–5(d)) [15]. Hence, the presence of C=O stretches in the modified cellulose buttresses the theory that the functionalization reagents are able to only penetrate the disordered, amorphous

regions and the polymer's surface [3]. That is, the chemical functionalization reactions are more likely to occur in these amorphous regions, neglecting the intracrystalline regions [3], resulting in the lack of intensity of the C=O stretch in the 1623 to 1780 cm^{-1} region of FTIR spectra. The network of hydrogen bonding also inhibits complete functionalization success.

Additionally, a ratio for the degree of substitution was determined using the O–H stretch visible between 4000 and 2995 cm^{-1}, which ideally will reduce with the modification of the primary and secondary hydroxyl groups located at the C2, C3, and C6 positions on the glucose monomers, and the C–C, C–OH, and C–H ring and side group vibrations. The ratio was determined using

$$\text{Ratio of Substitution} = \frac{\text{Neat Cellulose}}{\text{Functionalized Cellulose}} = \frac{I_{1046-994}/I_{4000-2995}}{I_{1046-994}/I_{4000-2995}}, \quad (1)$$

where $I_{1046-994}$ is the intensity range of the C–C, C–OH, and C–H ring and side group vibrations and $I_{4000-2995}$ is the OH stretch. Table 3 displays the ratio of the degree of substitution. For the nitric acid sample and its oxidized counterpart, the ratio of substitution was determined to be a 1 : 1 ratio, suggesting a nonsignificant change in the monomer backbone to the OH stretches from the neat to modified sample. Yet, the sulfuric acid and its counterpart display different characteristics, that is, a 2 : 1 ratio signifying a decrease in the OH stretch to the C–C, C–OH, and C–H ring and side group vibrations in the Albright-Goldman oxidized sample. Furthermore, comparative crystallinity indices were calculated to determine the degree of crystallinity (see Table 4).

For calculation of the indices (Table 4) from XRD, the height methodology was used, which tends to produce higher values when compared to other methods. The following equation was used to perform the percent crystallinity of the neat and modified samples:

$$\%\text{Crystallinity} = \frac{I_{\text{crystalline}}}{I_{\text{amorphous}} + I_{\text{crystalline}}} \times 100\%, \quad (2)$$

where $I_{\text{crystalline}}$ corresponds to the (002) crystalline peak located at approximately 2θ of 22.5° and $I_{\text{amorphous}}$ (I_{AM}) is the highest peak of the amorphous background region located at approximately 2θ around 18°. On the other hand, the crystallinity indices were calculated from FTIR spectra using

$$\%\text{Crystallinity} = \frac{A_{1423}}{A_{662}} \times 100\%, \quad (3)$$

where A_{1423} corresponds to the absorbance of the crystalline regions or H–C–H and O–H bending vibrations and A_{662} corresponds to the absorbance of the amorphous regions C–OH out-of-plane bending [13]. Even though the calculation methods are different, the percent crystallinity index was still greatest for the nitric acid extracted-modified sample but varied for the other samples. Yet, FTIR calculations tended to possess a less standard deviate, potentially being a more accurate measurement for crystallinity indices.

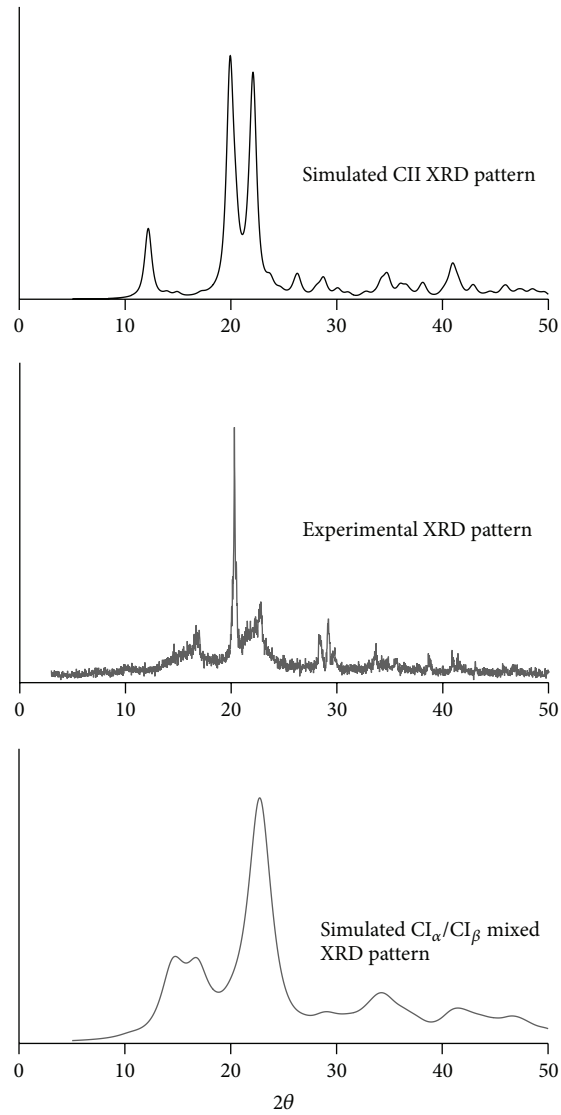

Figure 3: Simulated and experimental X-ray diffraction patterns revealing similar XRD peak patterns for the modified cellulose when compared to its mixed CI_α and CI_β and CII counterparts.

3.3. Scanning Electron Microscopy (SEM) Analysis. Figures 6(a)-6(b) show representative SEM images of the unmodified and modified cellulose structure and, apparently, reveal the effect of the chemical modification reaction on its shape, size, and dispersion factor. In the case of the unmodified cellulose, Figure 6(a), cellulose crystals with diameters and lengths on the micrometer scale can be observed. The micron-sized particles show similar rod-like shapes to that of the commercially purchasable microcrystalline cellulose, MCC, reported in earlier studies [15, 16]. The MCCs typically are produced from the acid hydrolysis of wood fibers and, as a result of hydrolysis techniques, aggregates of bundles of multisized cellulose microfibrils that are strongly hydrogen bonded to each other. The microfibrils are broken apart into smaller diameter mircocrystals (1–10 μm) before dissemination. Similar results can be seen in the sulfuric acid

Table 2: The peak wavenumber and the corresponding bonds of cellulose [14].

Peak wavenumber (cm^{-1})	Bonds	Modified	Nonmodified
4000–2995	OH-stretching	Observed	Observed
2883	C–H symmetrical stretching	Observed	Observed
1735 1384–1346	Hemicellulose	Not observed	Not observed
1640–1623	C=O, H–O–CH_2, and H–O–H bending of absorbed water	Observed	Observed (nitric) Not observed (sulfuric)
1600 1515 1426	Lignin aromatic Skeleton vibration	Not observed	Not observed
1423	H–C–H and O–H bending vibration	Observed	Observed
1314	CH_2 rocking vibration at C6	Observed	Observed
1046–994	C–C, C–OH, and C–H ring and side group vibrations	Observed	Observed
1205–895	COC, CCO, and CCH deformation and stretching	Observed	Observed
662	C–OH out-of-plane bending	Observed	Observed

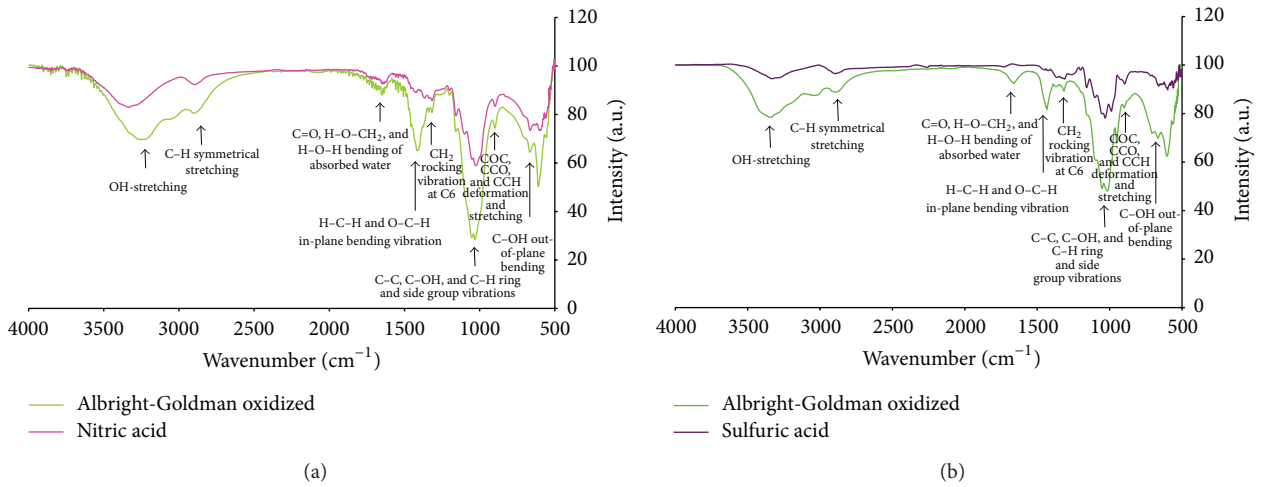

Figure 4: Fourier transform infrared spectroscopy (FTIR) spectra of nitric acid (a) and sulfuric acid (b) extracted cellulose and its Albright-Goldman modified counterparts.

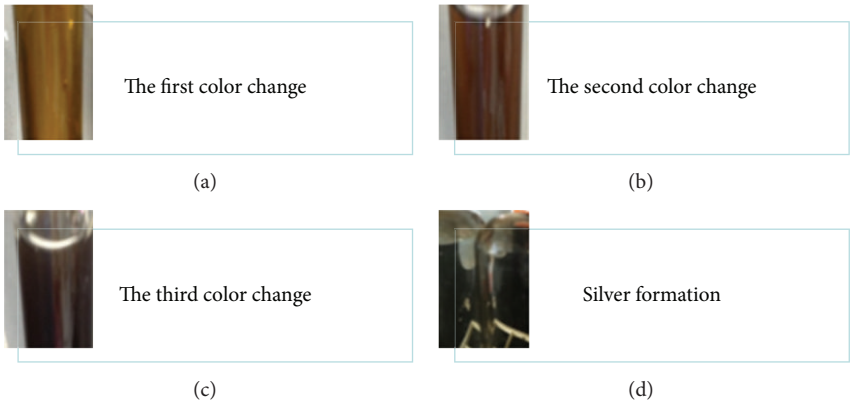

Figure 5: Tollens' test.

Table 3: The ratio of the OH stretch to the C–C, C–OH, and C–H ring and side group vibrations.

Sample	Bonds	Intensity range	Ratio of the nonmodified to modified
Albright-Goldman oxidized (nitric acid)	OH-stretching	33.06	1 : 1
	C–C, C–OH, and C–H ring and side group vibrations	74.23	
Nitric acid	OH-stretching	19.97	
	C–C, C–OH, and C–H ring and side group vibrations	43.95	
Albright-Goldman oxidized (sulfuric acid)	OH-stretching	21.62	2 : 1
	C–C, C–OH, and C–H ring and side group vibrations	51.97	
Sulfuric acid	OH-stretching	6.05	
	C–C, C–OH, and C–H ring and side group vibrations	22.26	

Table 4: The crystallinity indices for the neat nitric and sulfuric acid extracted samples and their Albright-Goldman oxidized counterparts.

Characterization technique	Nitric acid	Albright-Goldman (nitric acid)	Sulfuric acid	Albright-Goldman (sulfuric acid)
FTIR	43.61% ± 0.01	98.57% ± 0.01	29.76% ± 0.03	59.43% ± 1.11
XRD	71.88% ± 4.19	92.52% ± 2.26	70.58% ± 1.18	69.65% ± 5.39

hydrolysis of cellulose extracted from wheat straw. That is, due to the strong hydrogen bonding and extraction process, the presence of aggregation is apparent. However, there are individual MCC fibers present.

In contrast, Figure 6(b) shows a smoother clump of intertwined hydrolyzed cellulose microfibrils after modification using the Albright-Goldman oxidation reaction. A diameter less than 5 μm can be measured for all of the individual microfibrils and exhibits a rod-like shape with increased strain definition in the individual cellulose microfibrils structural orientation compared to the unmodified counterpart. This could be attributed to the disruption of the strong hydrogen bonding typically observed in the unmodified cellulose cases. That is, upon modification, the removal of the OH groups has allowed the cellulose crystals increased mobility in the absence of the force driven through that of hydrogen bonding. Yet, further analysis of how the Albright-Goldman oxidation reagents affect the appearance of the crystalline regions is necessary.

3.4. Thermogravimetric (TGA) and Modulated Differential Scanning Calorimetry Analyses (DSC). The TGA curves in Figure 7 show the thermal decomposition temperature of nitric and sulfuric hydrolyzed (HNO_3 and H_2SO_4) cellulose and cellulose samples that have undergone the Albright-Goldman oxidation reaction. Under both conditions, nitric or sulfuric cellulose modified using the Albright-Goldman oxidation reaction exhibits a more thermally stable structure as compared to that of the unmodified hydrolyzed cellulose samples. The HNO_3 modified samples apparently reveal a two-step decomposition reaction at temperatures around 200°C and 250°C, whereas the nitric acid sample begins to decompose around 300°C. It is well known that under the HNO_3 conditions nitro groups can be substituted onto the structure of the cellulose and, based on bonding energies, could cause the release of intermediates during the heating stages [17]. The typical bonding energies for formed O–N and O–S bonds are around 55 and 87 J/mol, respectively [18].

Furthermore, the derivative curve (Figure 6(b)) demonstrates the thermal rate of decomposition of neat nitric and sulfuric acid cellulose samples and the modified versions via the Albright-Goldman oxidation reaction. In region I, which is below 150°C, the nitric acid sample displays a slight peak attributed to water uptake, as previously observed in Figure 7(a). However, the neat H_2SO_4 and oxidized samples do not portray this peak. In region II—from 150°C to 550°C—the greatest rate of decomposition is observed for all the samples. The nitric-modified sample begins to decompose slightly above 200°C at rate of 0.6/°C; however, a second decomposition occurs at approximately 250°C, suggesting that the sample loses mass over a broad temperature range. On the other hand, the nitric acid sample does not decompose until a slightly higher temperature (approximately 300°C) than that of the modified version, but the sample loses the majority of its mass at this point, therefore, rendering the nitric acid sample thermally unfavorable. H_2SO_4 modified cellulose begins to decompose at approximately 240°C with several more decomposition peaks occurring at elevated temperatures (from 375 to 550 degrees Celsius). In comparison to the acid hydrolyzed and modified nitric celluloses, the H_2SO_4 modified cellulose exhibits the greatest amount of residue at elevated temperatures which is ideal for high-temperature applications.

Further support for the TGA analysis of sulfuric acid modified cellulose exhibiting the greatest thermal stability can be observed in the DSC analysis, Figure 8. In this case,

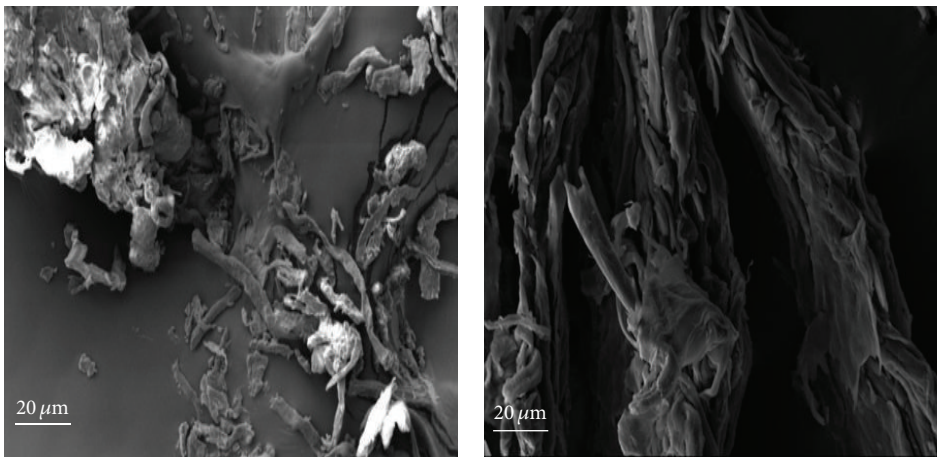

(a) (b)

Figure 6: SEM images of sulfuric acid extracted cellulose from wheat straw (a) and Albright-Goldman oxidized cellulose (b).

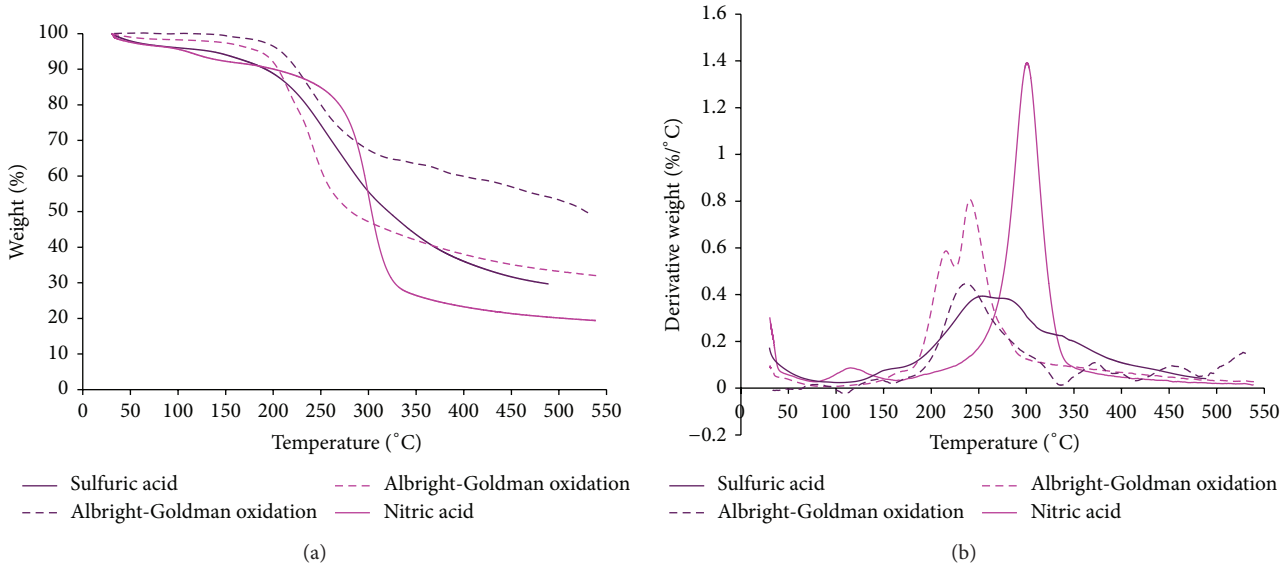

(a) (b)

Figure 7: Thermogravimetric (TG) weight loss and derivative curves of modified (a) and hydrolyzed (b) cellulose extracted from wheat straw.

the DSC analysis shows three distinct regions of thermal reactions—two endothermic reactions and one exothermic reaction. The first region is credited to water evaporation and occurs in the temperature range of 35°C to 130°C. In this region, the H_2SO_4 modified version also undergoes melting. The Albright-Goldman oxidized samples begin to melt at approximately 205°C and 200°C for the HNO_3 version. However, the nitric acid sample melts once at approximately 260°C and then completely degrades to form char at approximately 300°C (region 3), which is consistent with the TGA thermal analysis. The same behavior is prominent in the neat sulfuric acid sample but begins to melt at a temperature of around 230°C. However, the modified versions do not completely degrade to form char at a temperature of 400°C, making it ideal for elevated temperature applications.

4. Conclusions

In this study, we show that chemical functionalization of cellulose extracted from wheat straw displayed an altered crystal structure, signifying the start of structural rearrangements or the disruption of hydrogen bonding. That is, based on XRD spectra analysis, the modified cellulose exhibits structural arrangement that resembles that of a CII polymorph. However, the lack of an intense C=O stretch in the FTIR spectra leads to the fact that incomplete functionalization of the inner crystalline region occurred with functionalization mostly occurring on the outer amorphous regions. Yet, from the thermal analyses, the modified cellulose tended to have higher thermal stability and residual mass. Shifts in the char/degradation temperatures and heterogeneous melting

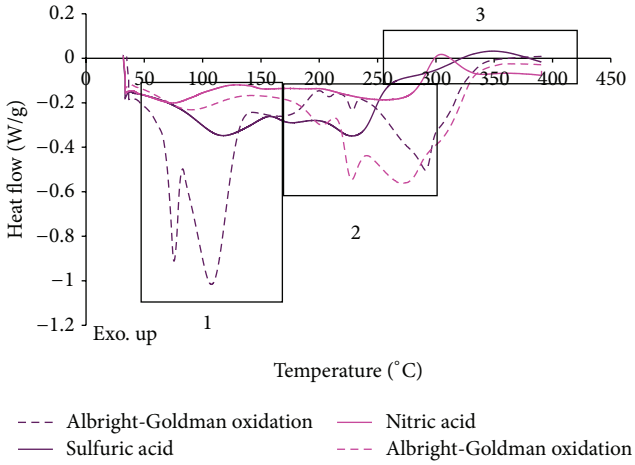

FIGURE 8: Modulated differential scanning calorimetry of functionalized and hydrolyzed cellulose extracted from wheat straw.

peaks also demonstrate the altered thermal behavior of the functionalized cellulose and its nonfunctionalized counterpart. However, the Jones oxidized samples were unable to be examined due to the lack of separation from the reduced chromium complex. To that end, it has been concluded in this study that the Albright-Goldman oxidation reaction can be used to chemically functionalize the cellulose without significant degradation of the cellulose structure or lowering of its thermal stability.

Conflict of Interests

The authors declare that there is no conflict of interests regarding the publication of this paper.

Acknowledgments

The authors gratefully acknowledge the National Science Foundation under Grant nos. NSF EPS-1158862, NSF HRD-1137681, and NSF IGERT on Sustainable Electronics DGE-1144843 for support of this research. The Department of Materials Science and Engineering and Department of Chemistry and Chemistry Center for Synthesis and Characterization are also recognized.

References

[1] J. Kim, G. Montero, Y. Habibi et al., "Dispersion of cellulose crystallites by nonionic surfactants in a hydrophobic polymer matrix," *Polymer Engineering and Science*, vol. 49, no. 10, pp. 2054–2061, 2009.

[2] A. Dufresne, *Nanocellulose: From Nature to High Performance Tailored Materials*, Walter de Gruyter, 2012.

[3] D. Klemm, B. Heublein, H.-P. Fink, and A. Bohn, "Cellulose: fascinating biopolymer and sustainable raw material," *Angewandte Chemie International Edition*, vol. 44, no. 22, pp. 3358–3393, 2005.

[4] D. T. Company, 2013, http://www.dharmatrading.com/cellulose.html.

[5] A. Buleon and H. Chanzy, "Single crystals of cellulose IVII: preparation and properties," *Journal of Polymer Science: Polymer Physics Edition*, vol. 18, no. 6, pp. 1209–1217, 1980.

[6] G. Tojo and M. I. Fernández, *Oxidation of Alcohols to Aldehydes and Ketones: A Guide to Current Common Practice*, Springer, New York, NY, USA, 2006.

[7] J. D. Albright and L. Goldman, "Dimethyl sulfoxide-acid anhydride mixtures for the oxidation of alcohols," *Journal of the American Chemical Society*, vol. 89, no. 10, pp. 2416–2423, 1967.

[8] T. Kondo and C. Sawatari, "A Fourier transform infra-red spectroscopic analysis of the character of hydrogen bonds in amorphous cellulose," *Polymer*, vol. 37, no. 3, pp. 393–399, 1996.

[9] NC State University, "Tollen's Test (Silver Mirror)".

[10] E. N. J. Ford, S. K. Mendon, S. F. Thames, and J. W. Rawlins, "X-ray diffraction of cotton treated with neutralized vegetable oil-based macromolecular crosslinkers," *Cellulose*, vol. 9, no. 11, pp. 18–23, 2010.

[11] A. D. French, "Idealized powder diffraction patterns for cellulose polymorphs," *Cellulose*, vol. 21, no. 2, pp. 885–896, 2014.

[12] *Cellulose*, 2014, http://www.wiley-vch.de/books/biopoly/pdf_v06/bpol6010_275_287.pdf.

[13] D. Ciolacu, F. Ciolacu, and V. I. Popa, "Amorphous cellulose—structure and characterization," *Cellulose Chemistry and Technology*, vol. 45, no. 1-2, pp. 13–21, 2011.

[14] M. Fan, D. Dai, and B. Huang, "Fourier transform infrared spectroscopy for natural fibres," in *Fourier Transform—Materials Analysis*, InTech, 2012.

[15] H. Chemar, K. Crews, A. Abdalla, A. Russell, and M. Curry, "Influence of strong acid hydrolysis processing on the thermal stability and crystallinity of cellulose isolated from wheat straw," *International Journal of Chemical Engineering*, In press.

[16] R. J. Moon, A. Martini, J. Nairn, J. Simonsen, and J. Youngblood, "Cellulose nanomaterials review: structure, properties and nanocomposites," *Chemical Society Reviews*, vol. 40, no. 7, pp. 3941–3994, 2011.

[17] R. P. Swatloski, S. K. Spear, J. D. Holbrey, and R. D. Rogers, "Dissolution of cellose with ionic liquids," *Journal of the American Chemical Society*, vol. 124, no. 18, pp. 4974–4975, 2002.

[18] Michigan State University, *Standard Bond Energies and Bond Dissociation Energies*, http://www.cem.msu.edu/~reusch/OrgPage/bndenrgy.htm.